Constructing and Pilot Testing a Novel Prostate Magnetic Resonance Imaging/Ultrasound Fusion Biopsy Phantom

Brandon Caldwell, David Greenwald, Daniel Moreira, Rong-wen Tain, Christopher Coogan, Karen Xie, Winnie Mar, Peter Pfanner, and Michael Abern

OBJECTIVE To describe the design and build of a novel phantom for magnetic resonance imaging (MRI)/ultrasound (US) fusion biopsy and present pilot testing results from a multicenter urology resident training session.

METHODS We cast our phantom from polyvinylchloride-plastisol that features 10 mm and 5 mm blue clay tumors, a urethral lumen, and an echogenic capsule. T2-weighted images were acquired with a 3T MR750 scanner (GE Healthcare, Boston, MA). Fusion testing was performed on the bkFusion system (BK ultrasound, Peabody, MA) with MIM Symphony software (MIM, Cleveland, OH) and an 18-gauge Bard Monopty disposable gun (Bard, Murray Hill, NJ). Twenty residents from 6 urology programs in Chicago performed proctored user testing.

RESULTS The per phantom material cost was $12. The phantom was compatible with all necessary equipment to create a MRI/US fusion data set. MRI and US imaging characteristics were excellent with hypointense lesions. Image fusion was achieved through both end and side fire ultrasound probes. The phantom allowed for biopsies to be performed, and target lesion hits were confirmed by visual inspection of core samples. 38% (8/21) of urology resident pilot testing participants had previously performed a fusion biopsy. The mean postsession survey scores were (1-10 [best]): realism 9.0, usefulness 9.4, ease of use 9.1, ease of orientation 8.9, and overall experience 9.3.

CONCLUSION This simple and inexpensive phantom allows for training and accuracy testing of MRI/US fusion biopsy hardware and software platforms. UROLOGY 124: 33–37, 2019. © 2018 Elsevier Inc.

Early detection of prostate cancer (PCa) is essential for optimal clinical outcomes; the gold standard for diagnosis is histopathologic assessment of transrectal ultrasound (TRUS)-guided systematic biopsy core samples.[1] Suboptimal grade accuracy and detection of anteriorly located PCa diagnosed from systematic biopsies has led to the growing implementation of TRUS-magnetic resonance imaging (MRI) fusion guided biopsies.[2-4] By targeting lesions on MRI, as compared to systematic biopsy, studies have shown increased detection of clinically significant tumors while decreasing the detection of indolent tumors.[5-7]

As MRI is increasingly integrated into the PCa detection paradigm, MRI fusion biopsy is an increasingly utilized procedure. While there are currently no required training programs or guidelines for this procedure for urologic trainees, we should anticipate increasing educational and training needs for procedure mastery. One widely utilized category of imaging training tools is phantoms, which are inanimate models that are designed to approximate standardized human tissues. Incorporating phantoms in ultrasound (US) training has been shown to be beneficial for learning clinically relevant skills, like obtaining useful images and identifying objects.[8] The use of phantoms can allow for training with no risk to human subjects.

Our goal was to find a phantom system for MRI/US fusion biopsy training. We followed a structured process we have developed in the University of Illinois at Chicago (UIC) Innovation Center Laboratory to determine the needs of the system and survey the suitability of existing phantom systems. This process involves identifying current technologies and materials available, and comparing them against desired specifications and feasibility. Commercially available fusion phantoms cost hundreds to thousands of dollars and did not meet the specifications we thought important for a training model—cost-

From the Department of Urology, University of Illinois at Chicago College of Medicine, Chicago, IL; the Campus Center for Neuroimaging, University of California Irvine, Irvine, CA; the Department of Urology, Rush University Medical Center, Chicago, IL; and the Department of Radiology, University of Illinois at Chicago College of Medicine, Chicago, IL

Address correspondence to: Brandon Caldwell, M.S., Department of Urology, University of Illinois at Chicago, 820 S Wood St CSN 515 M/C 955, Chicago, IL 60657. E-mails: bmc@uic.edu; b.caldwell110@gmail.com

Submitted: June 19, 2018, accepted (with revisions): October 15, 2018

effective, durable, and visual feedback on target hits. To overcome these obstacles, we describe the design and fabrication of a novel prostate phantom system for fusion biopsy testing and training. We determined its utility by pilot testing it with urologic residency trainees.

MATERIALS AND METHODS

Prostate Phantom Design and Construction

We developed a specification for an MRI/US fusion biopsy phantom with several requirements: (1) Good T2 weighted MRI imaging characteristics (hypointense tumors); (2) Good TRUS imaging characteristics including the accommodation of end or side fire rectal probes; (3) Targets of realistic size for clinically significant PCa; (4) Ability to fire a clinically available core needle device into the phantom; (5) Ability to determine a target hit with the unaided eye; (6) Inexpensive and reproducible; and (7) Durable to withstand several core biopsies. By surveying the published literature as well as commercially available prostate imaging phantoms, we found none that met our specifications.

We therefore designed and fabricated a novel prostate phantom designed for MRI/US fusion biopsy testing. Several of the raw materials described by Hungr et al were used for reference in building our prostate phantom and notably include the use of polyvinylchloride-plastisol (PVC-P) (M-F Manufacturing, Fort Worth, TX) and Toluidine Blue O (Sigma Aldrich, St. Louis, MO) in the construction process.[9] The phantom consists of 4 major components: the frame, a pressure plate, the prostate, and the phantom body. The components of the phantom are shown in Figure 1. The frame, shown in Figure 1A, is constructed from $\frac{1}{4}$ inch acrylic, which is clear, lightweight, and MRI compatible. There are two $4\frac{1}{2} \times 6\frac{1}{2}$ inch walls and two $4 \times 6\frac{1}{2}$ inch walls surrounding a $4\frac{1}{2} \times 4\frac{1}{2}$ inch base, and the top is open to accommodate a pressure plate. These walls are solvent welded together using acrylic cement (SCIGRIP, Durham, NC) to avoid the use of metal fasteners that would not be compatible with the MRI. Within one of the walls is a 3×4 inch opening for TRUS probe insertion and manipulation.

Although PVC-P can provide realistic deformation by an US probe, too much can be detrimental to rigid TRUS-MRI fusion registration methods. This compelled us to develop an adjustable pressure plate to allow for optimization of phantom deformation. A $3\frac{3}{4} \times 3\frac{3}{4}$ inch acrylic plate was created with protruding arms on top to hold Velcro fasteners. This plate is placed on top of the phantom, once inserted in the acrylic frame, and tightened with the Velcro to apply the desired vertical downward pressure, as determined by satisfactory TRUS image quality, onto the phantom as shown in Figure 1B.

A 50 cc hand molded prostate model was used to create a 2-part silicon injection mold, as shown in Figure 1C. A 100 mL PVC-P mixture is heated up to ~450°F in a glass beaker for 20-25 minutes to polymerize, and is poured into the bottom half of the mold. We then form 10 mm and 5 mm diameter synthetic spherical "lesions" from plastalina nonhardening clay (Van Aken, North Charleston, SC). Rather than using hardened clay like Hungr et al., we use realistically sized soft clay lesions so we can retrieve and identify biopsy cores upon hits. We place a 10 mm lesion in a marked location, indicated previously on the mold in ink, located in the left basal posterior of the prostate. We then attached the top half of the mold and pour additional PVC-P (~15 mL) without completely filling the mold. When the mold has cooled enough to hold form, the top half is removed, and we placed a 5 mm clay lesion in a marked location, again indicated from the mold, located in the right anterior apex of the prostate. After placing the 2 lesions, the top half is replaced, and we fill the rest of the mold with PVC-P and let it set for at least 30 minutes. Once the PVC-P prostate can be removed from the mold, it is placed in a water bath to expedite curing. The remaining PVC-P mixture, ~50 mL, is reheated to its liquid state and 0.5 g of Toluidine Blue O is mixed in, which will act to create an echogenic response from the material. We coat the previously casted prostate in the PVC-P/Toluidine Blue O mixture and place it in a water bath to cure.

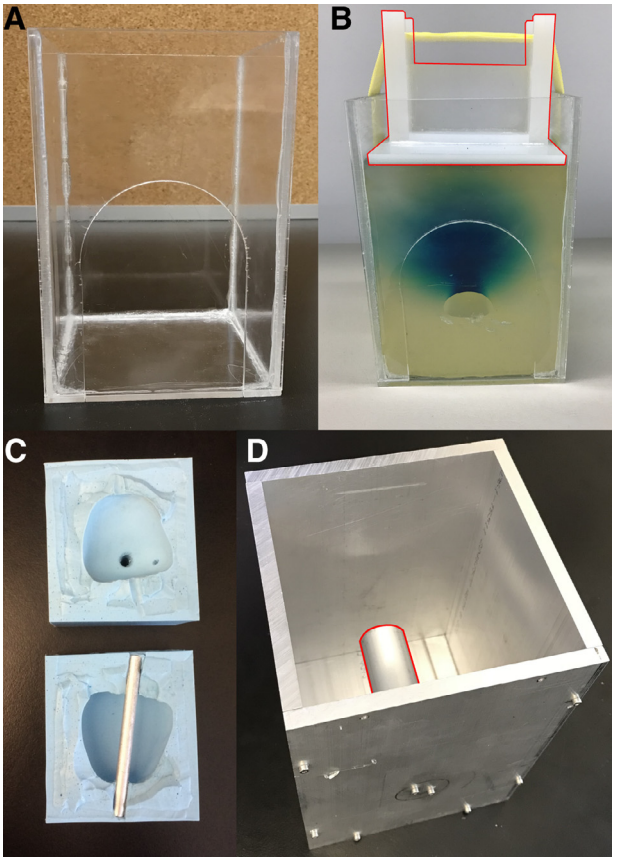

Figure 1. (**A**) Prostate phantom acrylic frame. (**B**) Assembled phantom with pressure plate highlighted in red. (**C**) Two-part silicon injection mold split along the coronal axis. (**D**) Aluminum mold for the phantom "body;" the aluminum column maintaining the rectal cavity is highlighted in red. (Color version available online.)

The phantom body is cast from a $\frac{1}{4}$ inch thick aluminum mold, as shown in Figure 1D, with a 4×4 inch base, two $4\frac{1}{2} \times 6\frac{3}{4}$ inch sides, and two $4 \times 6\frac{3}{4}$ inch sides. A 3 inch long by 1 inch diameter aluminum cylinder is used to maintain a rectal cavity within the phantom body for probe insertion. The cylinder, highlighted in Figure 1D, attaches to the center of 1 side, $2\frac{1}{2}$ inch from the base. We prepare 800 mL of activated PVC-P, as described above, and pour it into the aluminum mold to coat the affixed cylinder by ~2-3 mm, simulating the rectal wall. After allowing the PVC-P to cool, the prostate, cast in the 2-part silicone mold, is placed above the cylinder ~1 inch from the wall. An additional 800 mL of activated PVC-P is poured to fill the mold, which is left overnight to cool. The phantom,

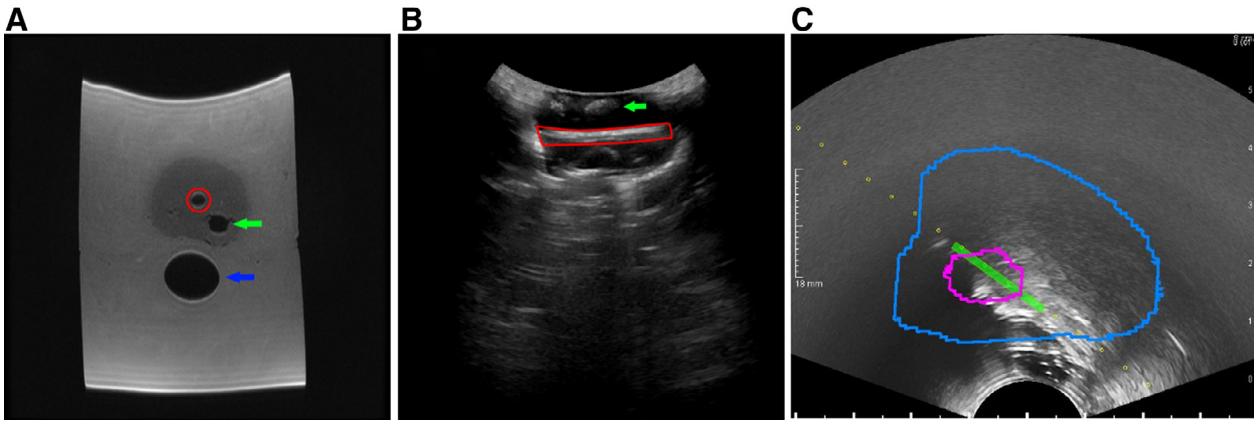

Figure 2. (**A**) Axial T2 weighted MR image of the constructed phantom. (**B**) Sagittal US of the phantom's "prostate" outside the phantom body. The lumen simulating the prostatic urethra is highlighted in red, the lumen simulating the rectum is noted with a blue arrow, and a lesion is denoted with a green arrow. (**C**) Sagittal view of prostate within phantom within fusion software. Lesion is marked in purple, core taken in green, prostate contour in blue. Image obtained post-training session — previous biopsy tracks (60+) visible. (Color version available online.)

once cooled, is now complete. It can be removed and placed into the acrylic frame with the pressure plate for use.

A step-by-step guide is provided in Supplement A.

Phantom MRI Data Acquisition and Processing

MR images of the phantom were acquired in the UIC Center for 3T Research, which contains a GE MR750 3T human scanner devoted to research (GE Healthcare, Boston, MA). T2 weighted images were acquired in the axial, sagittal, and coronal planes using a 32-channel cardiac coil as shown in Figure 2A. The image dataset was exported to DICOM format. The DICOM dataset was imported and prostate contour and tumors were annotated using the MIM Symphony Dx software (MIM, Cleveland, OH).

Pilot Fusion Biopsy Testing

An end-fire TRUS probe and the bkFusion system (BK ultrasound, Peabody, MA) were utilized to perform MRI/US fusion in the sagittal imaging plane. Participating residents introduced an 18-gauge, 20 cm long Bard Monopty biopsy gun (Bard, Murray Hill, NJ) through the TRUS probe to perform core biopsies of the phantom. Determination of a target hit was performed under direct visual inspection of the biopsy core material and was considered positive if any of the blue "tumor" material was seen in the core, as shown in Figure 3.

Twenty one urology trainees from six residency training programs in Chicago participated in the MRI/US fusion biopsy station during The Chicago Urological Society Resident Simulation Workshop and Competition in January 2018.[10] The participants were given a brief tutorial of the operation of the bkFusion system by urology faculty with extensive clinical experience with MRI/US fusion biopsies (MA). They were asked to locate the 2 tumors with TRUS and each participant was then allowed 2 biopsy attempts at the 10 mm tumor and 1 attempt at the 5 mm tumor. The 2 lesions were precontoured on the MRI for purposes of the fusion system, recreating a standard clinical encounter. After their 3 attempts, each participant completed an anonymous, nonvalidated survey. We recorded post graduate year, prior fusion biopsy experience, as well as ratings, on a 1-10 Likert scale (10 is best), of their experience with the session under the following categories: realism, usefulness, ease of use, ease of orientation, and overall experience. The full questionnaire is available in Supplement B.

RESULTS

Phantom Design

The constructed phantom produced desirable characteristics during MR and US imaging as illustrated in Figure 2A and 2B, respectively. Of note, the desired hypointense tumor signal is evident on the MRI T2-weighted images; the lesions do, however, appear on TRUS. During TRUS imaging, the prostatic capsule and urethral lumen are visible to allow for orientating the prostate in real

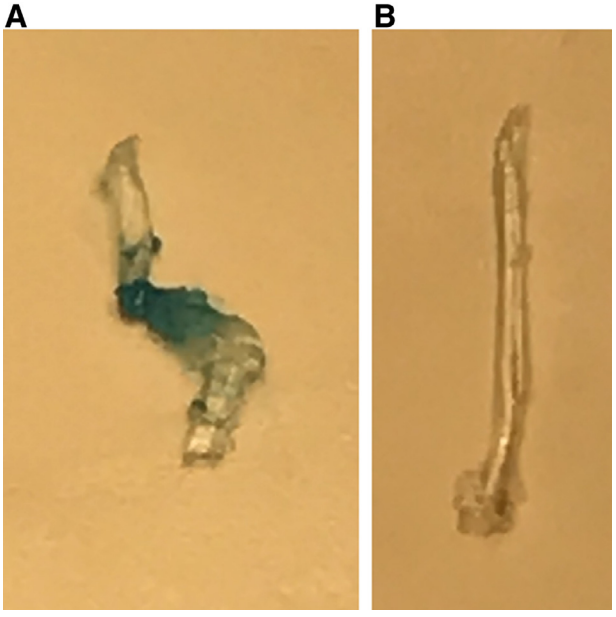

Figure 3. (**A**) Positive core from the phantom. (**B**) Negative core from the phantom. (Color version available online.)

time. The PVC-P of the prostate and surrounding allowed for successful penetration and function of the spring-loaded biopsy gun, and easy release of the material from the needle in preparation for repeat use. Total initial costs for building the phantom were $220, including materials for the molds and frame. The material cost for subsequent phantoms is $12.

Pilot Testing

Twenty one participants completed the pilot testing session. The participants were trainees from six Urology residency programs ranging from PGY 1 to 5 (mean 3.4 PGY). 38% (8/21) of the participants reported prior first hand fusion biopsy experience, with a range of 0-50 total biopsies performed. During TRUS imaging, 100% (21/21) of the participants were able to find at least one of the tumors, and 95% (20/21) were able to find both. When attempting fusion biopsy, 100% (21/21) of participants hit the 10 mm lesion in at least one of their 2 attempts, and 76% (16/21) were able to hit the 10 mm lesion on both attempts. Subsequently, 81% (17/21) of participants were able to hit the 5 mm lesion with their single attempt. The mean postsession survey scores were (1-10 [best]): realism 9.0, usefulness 9.4, ease of use 9.1, ease of orientation 8.9, and overall experience 9.3.

COMMENT

As MRI is increasingly utilized for the guidance of prostate biopsies, there is a need for physicians, both in residency and in practice, to be able to train on, practice with, and test fusion biopsy systems. To that end, phantoms are extremely useful. Commercial phantoms, however, cost in excess of $500 per unit. Despite their cost, commercial phantoms are unable to withstand repetitive biopsy needle punctures and we are unaware of any that can provide an indication of positive cores upon retrieval. At just roughly 2.4% of a commercial phantom's cost, we modified Hungr et al.'s method to create a phantom that provides satisfactory performance and durability for fusion biopsy training. Our model provides larger lesions, of size similar to those found in a clinical environment, which can be biopsied for hit verification with the naked eye; this provides a real-world approximation for clinical training and testing. Additionally, our model includes a pressure plate to mitigate elastic deformation and produce consistent clinically relevant fusion registration.

Before considering our phantoms value in research and training, they must meet practical considerations. By using common materials and a simple design, over 40 of our phantoms can be produced for the same cost as a single commercial phantom. Furthermore, our phantom is more durable. It can withstand over 60 core biopsy punctures with positive core detection, only being limited by the finite volume of the clay lesions. Realistic educational value is limited to ~15 biopsies per phantom due to the aggregation of needle tracks—a factor that increases the need for a cost-effect alternative to commercial models. We therefore establish feasibility in implementing these inexpensive and durable phantoms, which would not financially strain an institution, for research and training purposes.

The construction methods used allow one to create highly customized phantoms with reproducible results. Reproducing exact copies of the phantom enables the use of a single DICOM data set across all created phantoms for fusion biopsy procedures. For this study, the lesion locations we chose were intentional to provide an "easy" target, the 10 mm posterior lesion, and a "difficult" target, the 5 mm anterior lesion. Anterior lesions are often missed in standard biopsies, so their inclusion is paramount toward testing the efficacy of new techniques, technology, and for training physicians. The large lesion size resulted in high hit rates, but can be adjusted in future iterations. Other applications of this phantom model include comparative studies of fusion biopsy systems, software, and probe type (i.e., end-fire versus side-fire).

Our survey of residents from multiple institutions indicates that the phantom fusion biopsy training experience is outstanding, even without any prior experience. Although there was no observable association between experience and survey scores, it would make sense for users with less experience to benefit more from simulation training. Also, the soft clay lesions allow for biopsy cores to be inspected visually for immediate confirmation of a positive hit, which is critical for learner feedback. In addition to using phantom training to teach the procedure itself, other types of simulations can also be designed, like having trainees encounter common or uncommon complications that arise during the procedure such as being handed an uncocked biopsy gun. Training with a phantom is advantageous, because it allows physicians to become familiar with new instruments and techniques without having to worry about patient discomfort or mistakes. We also believe that physicians would be more willing to undergo additional simulation training with reasonably priced phantoms.

There are some limitations to the current phantom. As previously mentioned, while the phantom itself can hold up to multiple needle punctures, there is only so much clay within the embedded lesions from which one can biopsy. Additionally, upon repeated use, needle tracks appear and interfere with TRUS imaging. In this model, the embedded clay tumors are visible on TRUS—which is often not the case in clinical practice.[11] As this was a proof of concept and pilot study, we did not compare our phantom with other commercially available nor test on multiple fusion platforms. These are future directions for this system. Finally, it is unknown how phantom training shortens the learning curve or translates to higher accuracy in a clinical environment.

The success of our model presents an opportunity for future studies. The phantom can be applied toward testing fusion biopsy accuracy using parameters such as tumor size and location, imaging sequence, hardware and software platforms, longitudinal user performance, and associating performance with user experience. Additional considerations can

be made in the design to include additional landmark features, frame adjustment to allow template biopsy, and to improve the user experience.

CONCLUSION

We describe the design and construction of novel prostate phantom system for MRI/US fusion biopsy testing. As MRI becomes more integrated into PCa detection, a tool such as our phantom may prove useful for training and testing of fusion hardware and software platforms.

Acknowledgments. This work was funded in part by an anonymous donation to the University of Illinois at Chicago Department of Urology.

We acknowledge Andrew Graham and the UIC Innovation Center for their assistance in the construction of the phantom. We also acknowledge Robert Zumph and Assam Aziz from BK Fusion for providing the equipment necessary for pilot testing.

SUPPLEMENTARY MATERIALS

Supplementary material associated with this article can be found, in the online version, at doi:10.1016/j.urology.2018.10.029.

References

1. Mottet N, Bellmunt J, Bolla M. EAU-ESTRO-SIOG guidelines on prostate cancer. Part 1: screening, diagnosis, and local treatment with curative intent. *Eur Urol*. 2017;71:618. Available at: http://www.europeanurology.com/article/S0302-2838(16)30470-5/pdf. Accessed March 26, 2018.
2. Epstein JI, Feng Z, Trock BJ. Upgrading and downgrading of prostate cancer from biopsy to radical prostatectomy: incidence and predictive factors using the modified gleason grading system and factoring in tertiary grades. *Eur Urol*. 2012;61:1019. Available at: https://www.ncbi.nlm.nih.gov/pubmed/22336380. Accessed March 26, 2018.
3. Leite K, Camara-Lopes L, Dall'Oglio M. Upgrading Gleason Score in extended prostate biopsy: implication for treatment choice. *Int J Radiat Oncol Biol Phys*. 2009;73:353. Available at: https://www.sciencedirect.com/science/article/pii/S0360301608007773. Accessed March 20, 2018.
4. Nelson AW, Harvey RC, Parker RA. Repeat prostate biopsy strategies after initial negative biopsy: meta-regression comparing cancer detection of transperineal, transrectal saturation and MRI guided biopsy. *PLoS One*. 2013;8:e57480. Available at: http://journals.plos.org/plosone/article?id=10.1371/journal.pone.0057480. Accessed March 20, 2018.
5. Sonn G, Chang E, Natarajan S. Value of targeted prostate biopsy using magnetic resonance-ultrasound fusion in men with prior negative biopsy and elevated prostate-specific antigen. *Euro Urol*. 2014;65:809. Available at: https://www.ncbi.nlm.nih.gov/pmc/articles/PMC3858524/. Accessed March 26, 2018.
6. Filson C, Natarajan S, Margolis D. Prostate cancer detection with magnetic resonance-ultrasound fusion biopsy: the role of systematic and targeted biopsies. *Cancer J*. 2016;122:884. Available at: https://www.ncbi.nlm.nih.gov/pubmed/26749141. Accessed March 26, 2018.
7. Kasivisvanathan V, Rannikko E, Borghi M. MRI-targeted or standard biopsy for prostate-cancer diagnosis. *N Engl J Med*. 2018;378:1767–1777. Available at: https://www.nejm.org/doi/full/10.1056/NEJMoa1801993. Accessed June 10, 2018.
8. Yoo M, Villegas L, Jones D. Basic ultrasound curriculum for medical students: validation of content and phantom. *J Laparoendosc Adv Surg Tech*. 2004;14:374. Available at: https://www.ncbi.nlm.nih.gov/pubmed/15684785. Accessed March 26, 2018.
9. Hungr N, Long JA, Beix V. A realistic deformable prostate phantom for multimodal imaging and needle-insertion procedures. *Med Phys*. 2012;39:2031. Available at: https://www.ncbi.nlm.nih.gov/pubmed/22482624. Accessed December 10, 2016.
10. Chow AK, Sherer BA, Yura E. Urology residents' experience and attitude toward surgical simulation: presenting our 4-year experience with a multi-institutional, multi-modality simulation model. *Urology*. 2017;109:32–37. Available at: https://www.ncbi.nlm.nih.gov/pubmed/28801218. Accessed April 16, 2018.
11. Harvey CJ, Pilcher J, Richenberg J. Applications of transrectal ultrasound in prostate cancer. *Br J Radiol*. 2012;85:S3–S17. Available at: https://www.ncbi.nlm.nih.gov/pmc/articles/PMC3746408/pdf/bjr-85-S3.pdf. Accessed April 16, 2018.